

Conjugate solidification and melting in multicomponent open and closed systems

G. W. BERGANTZ

Department of Geological Sciences AJ-20, University of Washington, Seattle, WA 98195,
U.S.A.

(Received 10 September 1990 and in final form 25 March 1991)

Abstract—Motivated by phase change technologies of geological materials, the time-dependent conjugate solidification and melting of multicomponent materials are considered in one dimension with open and closed thermal convection. The scaling of the driving temperature difference for convection is a function of the temperature difference between the isotherm which delimits a rigid mush from a slurry, and the free stream temperature. The temporal evolution of the solid and mushy zones for the open system multicomponent case is qualitative similar to the single component case. Maximum heat transfer rates are as much as 1.35 times that of coupled, conductive solidification/melting. The convecting, closed system case yields two possible outcomes: a monotonic progression of solidification or an oscillation in the positions of the isotherms, depending on the ratio of the heat transfer coefficient to the enthalpy content and geometry of the fluid reservoir.

1. INTRODUCTION

THE FORMULATION and development of self-consistent transport models for multicomponent phase change is the subject of increasing attention. This is motivated by a variety of issues in applied and pure science: energy storage in phase change materials (PCM), the *in situ* vitrification (ISV) of hazardous waste, the engineering of geothermal heat exchangers, the assessment of volcanic hazards, and fundamental questions related to the origin and evolution of magmas. The dominant obstacle in the quantitative treatment of these strongly non-linear problems is that they often involve multicomponent materials and spatially dependent enthalpy changes; it is difficult a priori to predict the temporal distribution of crystals and liquid. In addition, many of the applications require consideration of conjugate, or coupled, solidification/melting systems. The purpose of this study is twofold: (a) to address complexities of solidification/melting of geological materials, and (b) to model the generic features of the scaling and transient, multicomponent, conjugate solidification and melting in a semi-infinite medium coupled to either an open or closed convecting fluid reservoir.

Recent reviews of the burgeoning literature on the heat and mass transfer attendant with phase change can be found in refs. [1–4]. Among the more notable contributions to the physiochemical theory of multicomponent phase change are the works of Hills, Roberts and Loper [5–11] and those from the group at Purdue University, e.g. refs. [12, 13]. There have also been a variety of laboratory experiments of multicomponent systems, typically salt solutions [1–3, 14, 15], in an attempt to identify some of the generic elements of the heat and mass transfer. The laboratory

experiments provide a qualitative means to investigate the diversity of fluid structures and macrosegregation, however, it is apparent that buoyancy is generated locally in a complex manner and hence, there are scaling problems when applying these experiments to systems of engineering and geological interest [13, 16]. In an effort to explore a wider parameter range, numerical methods have been applied to the problems of multicomponent phase change [13, 17, 18]. Although qualitative agreement is good, they do not agree with the laboratory experiments in all aspects of the macrosegregation and are also computationally expensive [13, 17].

Part of the difficulty lies in the continuum description of a crystal–liquid mush. To this end, Hills, Loper and Roberts make one important distinction in their work: the difference between a mush and a slurry. A mush is an assemblage of crystals with an interstitial melt phase; a slurry is a mixture where crystals are distributed in an expanse of melt. The term ‘mush’ will be used in this paper in the same spirit: to indicate an essentially rigid and porous region of crystals and melt. One key element in the mush–slurry distinction is that the transition from a mush to a slurry is a rheological one. The self-partitioning of a multi-phase system into regions of mush and convectable, mobile slurry was further explored in the axiomatic work of Brandeis and Marsh [19] who introduced the concept of the convective liquidus. The convective liquidus is defined as the temperature below which convection is weak or non-existent. A related concept originating in the metallurgical literature is the concept of the contiguity limit. Contiguity is a measure of solid–solid grain contact [20, 21] and the contiguity limit is the volume melt fraction at which a ‘rigid’ aggregation of crystals takes on suspension-like behavior. In the

NOMENCLATURE

a_n	coefficient in the polynomial representation of the solid fraction distribution, equation (10)	t	time
b	shape factor in temperature approximation, equation (12)	V	volume of material per unit area of cooling surface.
B	parameter group, equation (9)	Greek symbols	
c_p	specific heat capacity	Γ	parameter group defined in equation (25)
d	power of the temperature in the parametric treatment of convection, equation (20)	δ	thickness of the i th region
D	normalized difference between thickness of i th region in the multicomponent to single component case	Δ	dimensionless thickness of the i th region, equation (28)
f_s	solid fraction distribution	θ	dimensionless temperature, equation (8)
h	spatially averaged parameter group from heat transfer coefficient, equation (20)	κ	thermal diffusivity
k	thermal conductivity	ρ	density
L	specific latent heat	τ	dimensionless time, equation (8).
M_L	mass of melt per unit area of cooling surface	Subscripts	
Q	heat flux convecting melt	CL	convective liquidus
St	modified Stefan number	CR	country rock
T	temperature	CRS	country rock solidus
		L	liquid (melt)
		m0	initial melt values
		s	solid region
		0	value at time equal to zero.

geophysical literature this rheological transition is called the critical melt fraction [22, 23].

The actual value of the convective liquidus is often difficult to predict and there is very little unequivocal geological data to indicate what solid fraction corresponds to the convective liquidus [19, 21]. It will no doubt be a function of strain rate, liquid viscosity, gradient in volume percent melt, and the usual transport properties and, hence, composition. Based on a few experiments and geological observations the convective liquidus can be anywhere from the isotherm corresponding to a few percent crystals to about 50% [21, 23]. Knowledge of this parameter is critical in quantifying the heat transfer systematics in geological systems, particularly the ISV process, as magmas can simultaneously have regions that are behaving as mushes and as slurries. This is apparent upon examination of the products of geological activity, such as lava flows, where crystals commonly exist in a distributed fashion within a glassy or hypocrystalline matrix indicating heterogeneous nucleation and growth throughout the magma. Magmas (silicate melts) also solidify from the margins inward, as demonstrated by the Hawaiian lava lakes [24] and in many plutons; also see the discussion in ref. [25]. It is difficult to know the relative importance of processes operating in the mushy zone as opposed to the slurry in producing the chemical diversity seen in the geological record.

Geological systems differ from metallurgical systems in a number of ways. For example, the initial and boundary conditions and geometry may differ.

Magmas are rarely superheated, and nucleate heterogeneously at small undercoolings of $\sim 10^{-2}$ – 10^{-4} °C [26]. The boundary conditions are also different, magmas are usually surrounded by a semi-infinite conducting medium and hence the vigor of convection and progress of solidification in magmas will be modulated by the enthalpy transport processes in the adjoining 'country rock' [27, 28]. Depending on the degree of supercooling in the country rock, the degree of superheat in the magma, and the value of the convective liquidus, the magma may initiate melting in the country rock which itself could undergo a fluid instability and alter the time and length scales of the solidification process. The heat and mass transfer associated with this coupled process of solidification and melting constitutes a conjugate system.

The problem of conjugate solidification of a single component fluid in forced flow in pipes or molds has received some attention [4]. One important result from these works is that the thickness of the solid will change with time as a function of supercooling, superheating, style and duration of convection and composition. Conjugate heat transfer attendant with single component solidification or melting in the presence of natural convection has recently been treated by Bejan and co-workers [29–31]. They emphasize the dynamic nature and intrinsic time dependence of the length scales in conjugate phase change problems. Conjugate solidification and melting of multi-component systems has received very little attention and as demonstrated below can differ markedly from the single component case.

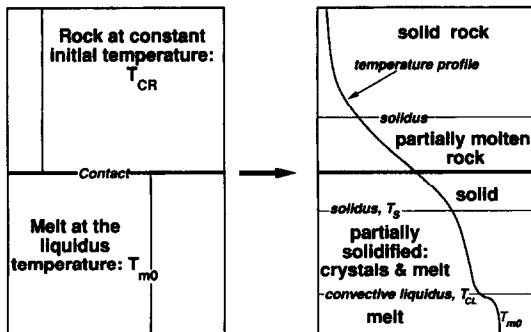


FIG. 1. Initial condition of coupled solidification/melting system. At time equal to zero, a well mixed melt is brought into contact with cold surroundings.

The focus of this contribution is to bring together a number of the issues considered above and to explore some of the generic aspects of the coupled system shown in Fig. 1 in a context that will have application to both the engineering of molten geological materials and the broader questions of scientific interest. This is the first of a number of reports detailing both numerical and experimental investigations of coupled solidification/melting of multicomponent materials.

2. PROBLEM FORMULATION

Consider a semi-infinite multicomponent solid initially at temperature T_{CR} which is below its melting temperature and suddenly brought into contact with a multicomponent fluid reservoir initially at temperature T_{m0} (Fig. 1). After some time the enthalpy transfer from the liquid reservoir to the solid may have initiated melting in the solid with concomitant solidification in the liquid. As both solid and liquid are multicomponent materials, but not necessarily of the same composition, the phase change process will yield regions of mixed solid and liquid phase on both sides of the original contact. The simultaneous propagation of the regions of melting and freezing comprise a conjugate system where the heat transfer systematics are intimately coupled to the degree of supercooling, superheating and physical chemistry. We will consider cases where the enthalpy content of the fluid reservoir is both finite and infinite. The heat transfer in the mushy zone will be assumed to be by conduction; convection in the all fluid portion will be treated by invoking a heat transfer coefficient formulation.

Using a conduction equation to describe the heat transfer in the mushy zone has some justification based on the work of refs. [32–35] where it is argued that the Peclet number for flow in the mush is much less than 1. Although a number of numerical and experimental models of the solidification of salt solutions show rather remarkable degrees of macro-segregation driven by double-diffusive convection [13,

14, 17], we are assuming that, to first order, this global redistribution is locally negligible with regard to the heat transfer. This assumption may be a good one for the geological case where melt viscosities can be very high and hence interdendritic flow may be an inefficient means of heat transfer [36–38], or for systems where the change in liquid density due to the selective removal of components into the solid phases may be small.

A general expression for the heat transfer in both the regions of melting and solidification is

$$\frac{\partial T}{\partial t} = \frac{k}{\rho c_p} \frac{\partial^2 T}{\partial x^2} + \frac{L}{c_p} \frac{df_s(T)}{dt} \tag{1}$$

The source term in equation (1) accounts for the latent heat effects as a function of temperature by the change of the volume solid fraction, $f_s(T)$. This form of the heat equation for mushy zone evolution is obtained by writing the energy equation in terms of the primitive variable enthalpy and then decomposing the enthalpy expression into the sensible and latent heat contributions as discussed in refs. [35, 39, 40]. Additional complexity can be introduced by writing the heat capacity and thermal conductivity in equation (1) as functions of the solid fraction.

The structure of equation (1) allows the usual similarity variable formulation [41] regardless of the form of $f_s(T)$; if the volume percent solid fraction has a non-linear dependence on temperature then the resulting ordinary differential equation is non-linear. This simplification is used in refs. [39, 42] to solve conjugate solidification problems in the absence of convection.

The method of weighted residuals is used here to solve the governing equations given below and the interested reader is directed to refs. [43, 44]. The basic procedure is to expand the solution in a set of trial and weighting functions, the weighting function chosen such that an inner product with the weighting function over one of the independent variables is zero. If the weighting function is taken as unity, one obtains the integral method of Goodman [45].

Figure 2 shows a variety of solid fraction dis-

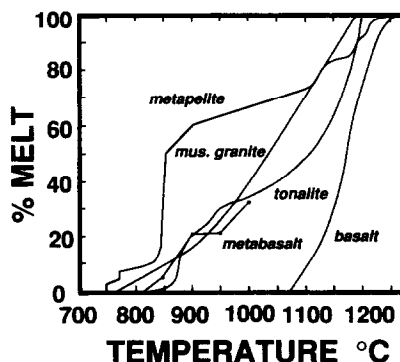


FIG. 2. Melt fraction distributions for some common rocks.

tributions for commonly occurring rock types. The curves need not be smooth or continuous: as phases are consumed or new phases become stable, the slope of the solid fraction curve will change. The presence of invariant points, such as eutectics, will yield jumps in the solid fraction distribution. The methodology adopted here was to subdivide the solution domain into regions delimited by isotherms wherein the solid fraction distribution curves are continuous. The isotherms can be chosen such that jump conditions in the solid fraction distribution occur at the edge of a subdomain i . Thus, equation (1) yields a series of coupled equations of the form

$$\frac{\partial T_i}{\partial t} = \frac{k_i}{\rho_i c_{pi}} \frac{\partial^2 T_i}{\partial x^2} + \frac{L_i}{c_{pi}} \frac{df_{si}(T_i)}{dt} \quad \delta_{i-1}(t) \leq x \leq \delta_i(t) \quad (2)$$

$$-k_{i-1} \frac{\partial T_{i-1}}{\partial x} \Big|_{\delta_{i-1}} = -k_i \frac{\partial T_i}{\partial x} \Big|_{\delta_{i-1}} - (\rho_i L_i \Delta f_{s_{i-1}}) \frac{d\delta_{i-1}}{dt} \quad (3)$$

$$-k_j \frac{\partial T_j}{\partial x} \Big|_{\delta_j} = - \left[Q(t) + \frac{d\delta_j}{dt} (\rho_j L_j \Delta f_{s_j} + \rho_j c_{pj} (T_m(t) - T_{CL})) \right] \quad (4)$$

where equation (3) provides for the continuity of heat across adjacent subdivisions where the last term on the right-hand side accounts for jumps in the solid fraction distribution and equation (4) gives the flux at the j th interface between the mushy zone and the fluid reservoir. The first term on the right-hand side of equation (4) is the time-dependent flux associated with either free or forced convection and whose specific form will depend on both the extensive and intensive variables as well as the geometry. The next terms in equation (4) account for heat transfer associated with the moving interface: the enthalpy change associated with solidification and a term to account for the virtual suction experienced by an interface which is moving in a fluid with a different temperature. Note that in equation (2) the domain is moving as the positions of the bounding isotherms themselves are unknown. A similar methodology has been previously employed by Voller [39, 46].

Equation (2) can be recast as

$$\frac{\partial \theta_i}{\partial \tau} = B_i \frac{\partial^2 \theta_i}{\partial x^2} + \frac{1}{St_i} \frac{df_{si}(\theta_i)}{d\tau} \quad (5)$$

$$\theta_i(\delta_i, \tau) = 1, \quad \theta_i(\delta_{i-1}, \tau) = 0 \quad (6)$$

$$\frac{\partial \theta_i}{\partial x} \Big|_{\delta_i} = \frac{k_{i-1}(T_{\delta_{i-1}} - T_{\delta_{i-2}})}{k_i(T_{\delta_i} - T_{\delta_{i-1}})} \frac{\partial \theta_{i-1}}{\partial x} \Big|_{\delta_{i-1}} - \frac{(\rho_i L_i \Delta f_{s_{i-1}})}{k_i(T_{\delta_i} - T_{\delta_{i-1}}) \kappa_s^2 (T_{CL} - T_{CR})^2} \frac{d\delta_{i-1}}{d\tau} \quad (7)$$

where

$$\theta_i = \frac{T_i - T_{\delta_{i-1}}}{T_{\delta_i} - T_{\delta_{i-1}}}, \quad \tau = \frac{Q_0^2 \kappa_s}{k_s^2 (T_{CL} - T_{CR})^2} t \quad (8)$$

$$B_i = \frac{k_s^2 (T_L - T_{CR})^2}{Q_0^2 \kappa_s} \kappa_i, \quad St_i = \frac{c_{pi}(T_{\delta_i} - T_{\delta_{i-1}})}{L_i} \quad (9)$$

The characteristic length scale that appears implicitly in τ and B_i warrants some discussion. One of the fundamental features of conjugated heat transfer in semi-infinite domains, where the thermal potentials are specified in the far-field rather than at the interfaces between the coupled systems, is that the characteristic length scale is time dependent and hence a priori unknown and represents one of the degrees of freedom in the quantitative treatment of the problem. The implication of this is that the system is intrinsically time dependent. Melting and/or solidification problems also share this feature: the length scale associated with the thermal resistance across a growing region of mixed phase is coupled in a non-linear way to the driving thermal potentials. The length scale chosen here reflects a matching of the initial thermal loading due to convection at the edge of the mushy zone, Q_0 , and the heat carrying capacity associated with the system supercooling relative to the conductivity temperature product at the edge of the mush, $k_s(T_{CL} - T_{CR})$.

Once $f_{si}(T_i)$ and a set of trial functions for $\theta_i(x, \tau)$ are given, the mathematical reduction of equation (5) can proceed. A generic expression for the solid fraction as a function of temperature across the i th subdivision can be obtained by invoking a polynomial approximation in T_i

$$f_{si}(T_i) = \sum_{n=0}^m a_n \left(\frac{T_i - T_{\delta_{i-1}}}{T_{\delta_i} - T_{\delta_{i-1}}} \right)^n = \sum_{n=0}^m a_n (\theta_i)^n \quad (10)$$

where the choice of a_n can be obtained by a curve fitting procedure. We note that

$$\frac{df_{si}(\theta_i)}{d\tau} = \frac{1}{(T_{\delta_i} - T_{\delta_{i-1}})} \frac{\partial \theta_i}{\partial \tau} \sum_{n=0}^m n a_n (\theta_i)^{n-1} \quad (11)$$

The temperature is assumed to be adequately represented by a second-order polynomial

$$\theta_i(x, \tau) = \frac{x - \delta_{i-1}}{\delta_i - \delta_{i-1}} + b_i(\tau) \left(\frac{x - \delta_{i-1}}{\delta_i - \delta_{i-1}} \right) \left\{ 1 - \frac{x - \delta_{i-1}}{\delta_i - \delta_{i-1}} \right\} \quad (12)$$

where

$$\frac{\partial \theta_i}{\partial x} = \frac{1}{(\delta_i - \delta_{i-1})} \left\{ 1 + b_i(\tau) \left[1 + 2 \left(\frac{x - \delta_{i-1}}{\delta_i - \delta_{i-1}} \right) \right] \right\} \quad (13)$$

Next, equation (5) is integrated with respect to the spatial independent variable which yields an expression of the form

$$\frac{d}{d\tau} \left\{ \int_0^{\delta_i - \delta_{i-1}} \left[\xi(C_1 - C_2\xi) \left[1 - \frac{1}{St_i} \sum_{n=1}^m a_n \xi^{n-1} (C_1 - C_2\xi)^{n-1} \right] \right] dx - \delta_i \left(1 - \frac{1}{St_i} \sum_{n=1}^m a_n \right) \right\} = B_i \left(\frac{\partial \theta_i}{\partial x} \Big|_{\delta_i} - \frac{\partial \theta_i}{\partial x} \Big|_{\delta_{i-1}} \right) \quad (14)$$

where

$$\xi = x - \delta_{i-1}, \quad C_1 = \frac{1}{(\delta_i - \delta_{i-1})} + b_i, \quad C_2 = \frac{b_i}{(\delta_i - \delta_{i-1})}. \quad (15)$$

Upon integration, the exact form of equation (10) will depend on m , the number of terms taken in the polynomial approximation to the solid fraction distribution. For example, if $m = 2$ equation (10) yields

$$\frac{d}{d\tau} \left\{ (\delta_i - \delta_{i-1}) \left[\frac{1}{2} - \frac{1}{St_i} \left(\frac{a_1}{2} + \frac{a_2}{3} \right) \right] + b_i (\delta_i - \delta_{i-1})^2 \left[\frac{1}{6} - \frac{1}{St_i} \left(\frac{a_1}{6} + \frac{a_2}{6} \right) \right] - \frac{1}{St_i} \frac{a_2 b_i^2 (\delta_i - \delta_{i-1})^3}{30} - \delta_i \left(1 - \frac{1}{St_i} \sum_{n=1}^m a_n \right) \right\} = 2B_i b_i. \quad (16)$$

The equations for the temperatures about the contact zone where $i = 1$ (see Fig. 1) require additional discussion. In the absence of convection the contact temperature will be constant in time; if convection is present, the temperature at this contact will change and becomes an additional dependent variable. The dimensionless contact temperature is defined as

$$\theta_1(\tau) = \frac{T_l - T_{\delta_{j+1}}}{T_{\delta_1} - T_{\delta_{j+1}}} \quad (17)$$

and the polynomial expression for $\theta_1(x, \tau)$ is

$$\theta_1(x, \tau) = \theta_j + \frac{(1 - \theta_j)x}{\delta_1} + b_1(\tau)x \left\{ 1 - \frac{x}{\delta_1} \right\}. \quad (18)$$

The value of the solid fraction at the contact will also be a function of time and hence an iterative scheme is required to ensure that the solid fraction is consistent with the contact temperature. Upon differentiation, equation (14) gives a set of initial value, coupled, ordinary differential equations with explicit dependent variables θ_i , δ_i , δ_{i-1} . The implicit dependence on values of δ down the thermal gradient from region i appear through the presence of b_i

$$\frac{db_i}{d\tau} = \frac{\partial b_i}{\partial \theta_i} \frac{d\theta_i}{d\tau} + \sum_{k=1}^i \frac{\partial b_i}{\partial \delta_k} \frac{d\delta_k}{d\tau}. \quad (19)$$

The b_i or 'shape functions' are found from the requirement of continuity of flux at the interfaces between each i th subdivision as given by equation (7).

2.1. Specification of the solid fraction distribution

The specification of the solid fraction distribution (10) requires an equilibrium phase diagram or phase equilibria laboratory experiments. If the phase diagram is available, the 'lever rule' is typically applied to yield the solid fraction as a function of temperature; an additional and often encountered assumption is that the liquidus curve is linear. Implicit in this practice is that some degree of equilibrium is assumed and that the rate controlling steps can be identified. Examples and discussions of the expressions for the solid fraction distribution have been given by Clyne and Kurtz [47], and Hills and Roberts [6] and are based on a modified form of the Scheil equation. Unlike the metallurgical systems of engineering interest, geological systems display a wide variety of solid fraction distributions as can be seen in Fig. 2, where the number of phases can be up to six or more.

An additional, and important, consideration is that the solid fraction during melting may not be a simple reversal of the solidification curves as the crystals may be zoned and hence present a changing compositional face as melting proceeds [7, 10]. In addition, volatile constituents may exist metastably in the form of structurally bound water in the inosilicates and phyllosilicates and upon melting yield large jumps in melt percentage over small temperature intervals as seen in Fig. 2. A heterogeneous spectrum of crystal sizes will also influence the rate at which melting proceeds [48]; this has been observed in the *in situ* vitrification field experiments where cobble size clasts behave as refractory components and can have a profound effect on the geometry and heat transfer systematics of the melt pool. Finally, caution must be exercised when using the $f_{si}(T_i)$ obtained from experimental data, such as that in Fig. 2, in transport models. These curves are constructed by interpolating between data points that represent discrete experiments where it is implicitly assumed that the kinetics of passing from one experimentally determined value of the solid fraction to the next along the $f_{si}(T_i)$ curve are negligible.

2.2. Parameterization of the convection in the liquid region

The time dependence of the convective contribution, $Q(t)$, in equation (4) has three components. The first is related to the boundary layer rise time which represents the time it takes for the fluid boundary layer to become two-dimensional everywhere and to adjust itself to changes in the geometry of the fluid reservoir as melting proceeds; this has been treated in some detail by refs. [29–31]. The second follows from the fact that the cold thermal reservoir is a semi-infinite medium, hence the thermal wave propagating outward into this initially supercooled domain will never reach a boundary of fixed thermal potential [29]. The third cause of time dependence follows from the nature of the initially warm fluid reservoir: for a system with a finite enthalpy content, the driving temperature difference in $Q(t)$ will decay. If one wall

is heated, or thermally forced, as in the examples considered by refs. [29–31], then the enthalpy content of the warm fluid reservoir is essentially infinite. While this is a good assumption for many scenarios of engineering interest, geological cases are probably better represented by a closed system. We will consider both cases here. We will ignore time dependence associated with the first of the components given above: it is assumed that the convective structures have an infinitely fast rise time and hence the length scales in the heat transfer coefficient are not explicitly time dependent.

The expression for the flux at the edge of the mushy zone in the fluid reservoir is

$$Q(t) = \bar{h}(\Delta T(t))^d \quad (20)$$

where \bar{h} is a spatially averaged parameter group whose form will depend on the reservoir geometry and assumptions regarding the state of the flow: laminar or turbulent, free or forced, etc. The constant Q_0 that appears in equations (8) and (9) above is the value of $Q(\tau)$ at $\tau = 0$.

The temperature difference appearing in equation (20) requires some discussion. It is apparent that it will be the temperature difference between the mixing cup temperature of the fluid reservoir, which may be time dependent, and the temperature at the mushy zone–fluid interface, δ_j . Recall that the temperature difference appearing in equation (20) is that between the fluid reservoir and the convective liquidus [19].

For the closed system calculations, the fluid temperature itself will be time dependent: natural convection will lead to cooling of the melt pool. The dimensionless form of the well mixed fluid temperature is

$$\theta_m(\tau) = \frac{\overline{T_m} - T_{CL}}{T_{m0} - T_{CL}} \quad (21)$$

where the overbar in equation (21) indicates average quantities. The expressions for the total solid and liquid per unit area at any time are given by

$$V_s(\tau) = \sum_{i=1}^{j-1} \int_{\delta_i}^{\delta_{i+1}} f_s(\theta_i) dx \quad (22)$$

$$V_L(\tau) = \delta_j - V_s \quad (23)$$

and the conservation of energy in the fluid gives an expression for the change of the interior temperature due to heat loss out through the combined solidification/melting system

$$\frac{d\theta_m}{d\tau} = -\Gamma \frac{\theta_m^d}{\left\{ 1 - \left[\frac{V_s}{M_L} (\rho_s - \rho_L) + \frac{\rho_s}{M_L} \delta_j \right] \right\}} \quad (24)$$

where

$$\Gamma = \frac{k_s^2 (T_{CL} - T_{CR})^2 \bar{h} (T_{m0} - T_{CL})^{d-1}}{Q_0^2 k_s c_{pL} M_L} \quad (25)$$

Key assumptions in using equation (24) to describe

the changing reservoir temperature are that the value of h and d are not time dependent and that the appropriate values can be predicted. Note that in using equation (24) we are *prescribing* the heat transfer systematics of the fluid reservoir, via equation (20) and so are introducing a degree of freedom that does not exist in real systems undergoing natural convection. This is not a trivial point and some controversy exists as to the length scales in solidifying, convecting fluids surrounded by a conducting medium; this is discussed at some length in refs. [16, 25].

Consideration of the dynamics of the mush itself, which may be prone to Rayleigh–Taylor or other types of instabilities as a function of geometry and crystal content, is beyond the scope of this treatment. It has been considered recently by refs. [16, 49]. These types of instabilities may ultimately prove to be important in the heat and mass transfer of magma bodies and represents a rich field of potential research in the dynamics of multi-phase flow.

3. NUMERICAL RESULTS

The system of coupled initial value ordinary differential equations that follows from equations (14) and (24) was solved numerically using the LSODE algorithm developed at Lawrence Livermore National Laboratory and available for general distribution [50]. The formulation was tested by solving the problem of single component solidification cooled by an infinite medium, for which the analytical solution is well known. The numerical results agreed to within 99.5% of the analytical solution for the position of the solidification front and the interface temperature. The singularities in flux that occur at time equal to zero+ were accommodated by prescribing a small initial distribution of the isotherms as given by the analytical solution obtained in the absence of convection. Numerical experiments revealed that the final results were insensitive to these initial offsets.

Due to the large number of thermophysical parameters and the variety of solid fraction distributions (Fig. 2) it is difficult to generalize the results, a point well made in ref. [17]. In an effort to identify the generic aspects of the system shown in Fig. 1, we will consider systems where all the thermophysical properties are the same and have linear solid fraction distributions. The solid fraction distribution for the country rock and melt are respectively

$$\begin{aligned} f_{SCR}(T^*) &= 1.0 - 2.0T^* & 0 \leq T^* \leq 0.5 \\ f_{SM}(T^*) &= 3.33(1 - T^*) & 0.7 \leq T^* \leq 1.0 \end{aligned} \quad (26)$$

where

$$T^* = \frac{T - T_{CRS}}{T_{m0} - T_{CRS}} \quad (27)$$

For the simulations detailed below, the global Stefan

number, equation (9), is 2 and the ratio of the difference between T_{CR} and T_{CL} , and T_{m0} is 100. More complex cases will be the subject of future communications.

3.1. Open system calculations

The open system results detailed below are appropriate for conditions where the enthalpy content of the fluid reservoir is essentially infinite and hence the thermal flux at the edge of the mushy zone is not time dependent: $Q(\tau) = Q_0$. This might occur during pipe flow or in enclosures where some of the bounding surfaces are constantly heated. Thus the conjugate solidification/melting system is the coupling of two semi-infinite reservoirs and the thermal wave travelling outward from the melt will not reverse direction, nor is a true steady state possible.

The evolution of the coupled solidification/melting system can be appreciated by examining the position of the solidus on both the melt and country rock sides and the position of the convective liquidus in the solidifying region. The dimensionless thickness of the i th region is given by

$$\Delta_i = \frac{Q_0 \delta_i}{k_s (T_{CL} - T_{CR})} \quad (28)$$

Figure 3 illustrates the temporal evolution of the regions of solid and mush where Δ_S is the position of the solidus, Δ_{CL} the position of the edge of the mush as defined by the convective liquidus, and Δ_{CRS} the position of the solidus in the country rock. The multicomponent system yields the same type of time dependence reported elsewhere for single component systems: early solidification followed by a retreat of the isotherms as the heat carrying capacity of the cold thermal reservoir is diminished in the face of a constant thermal loading, Q_0 . One important difference is that some solid remains as the convective liquidus isotherm is almost stationary throughout much of the

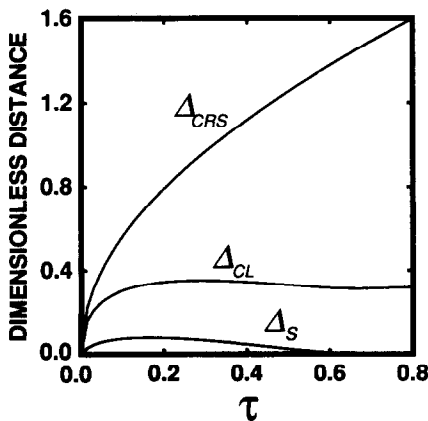


FIG. 3. Positions of the solidus in the initially molten region, country rock and the position of the convective liquidus, open system case, equation (28).

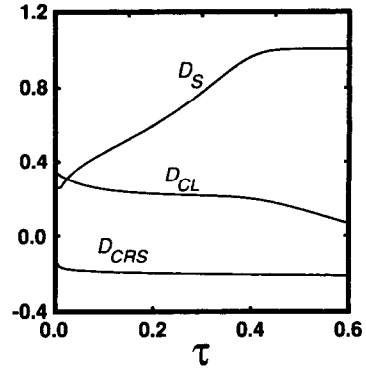


FIG. 4. Normalized differences between the computed positions of the solidus in the initially molten region, the country rock and the convective liquidus for the multicomponent vs the single component case, equation (29).

interval when the solidus isotherm is retreating. The position of the solidus in the country rock moves outward monotonically. Although the numerical results are shown only for the time period where the solidus isotherm cycles back to the contact, ultimately the contact temperature will reach the free stream temperature, T_{m0} , if the thermal conductivities are the same.

One measure of the difference between single and multicomponent systems is the difference between isotherms normalized to the multicomponent position. This difference D_i is defined as

$$D_i = \frac{\Delta_{iMULTI} - \Delta_{iSINGLE}}{\Delta_{iMULTI}} \quad (29)$$

where a value of zero indicates that the two systems give the same results and a value of one that the multicomponent case differs substantially from the single component case. For the parameter range considered, the multicomponent case differs notably from the single component case as shown in Fig. 4. This is attributable to the fact that having a multicomponent system is equivalent to an increased effective heat capacity.

The ratio of the thermal flux at the contact in the presence of convection to that of conduction yields an effective Nusselt number. This is plotted in Fig. 5. The maximum attainable value of this ratio is two [16] as conduction in the country rock provides the rate limiting step. Although the heat flux at the contact is decreasing with time, the ratio of convective to conductive heat transfer is increasing in the time period over which the solidus isotherm cycles back to the contact.

3.2. Closed system calculations

The closed system calculations have a more complex time dependence than the open system case, as it is the coupling of a finite melt reservoir with a semi-

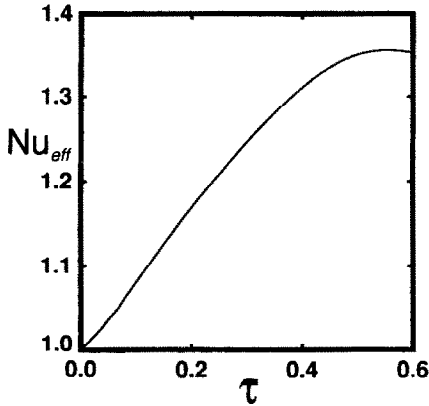


FIG. 5. Effective Nusselt number : ratio of thermal flux at the contact with convection to that where the melt reservoir is cooling by conduction only.

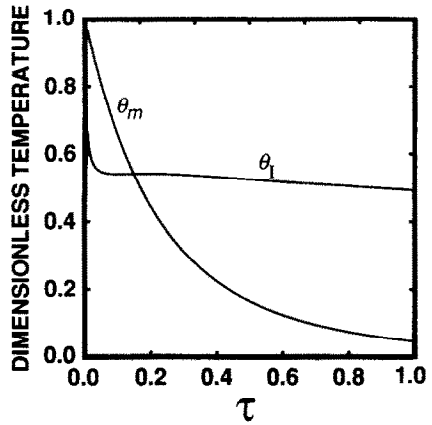


FIG. 7. Dimensionless temperature of the closed system melt reservoir and the dimensionless contact temperature, equations (21) and (17). $\Gamma = 0.88$.

infinite expanse of country rock. The thermal wave will pass out from the melt body and then undergo reversal as the cold reservoir temperature, T_{CR} , ultimately recovers to a steady state. We consider only that portion of the thermal history when the melting front is still propagating outward into the country rock.

Depending on the value of \bar{h} (and hence Γ), two scenarios are possible: for small values of \bar{h} , the progress of solidification is monotonic. This is shown in Fig. 6 as given by the position of the melt solidus Δ_S , convective liquidus Δ_{CL} and country rock solidus Δ_{CRS} . The convection in the melt decays before the cold thermal reservoir becomes thermally swamped and so there is no back melting from thermal loading as in the open system case. The dimensionless contact temperature and melt reservoir temperature are shown in Fig. 7. The contact temperature decreases continuously even while convection is

occurring. The temperature difference between the melt reservoir and the convective liquidus falls off to 1/e of the original difference at a dimensionless time of ~ 0.25 .

For a larger value of \bar{h} the progress of solidification undergoes an oscillation like that seen in the open system case. The convective thermal flux from the decay of the temperature difference between T_{m0} and T_{CL} is sufficient to initiate melting back as before, but stops before the solidus isotherm retreats back to the original contact, this is shown in Fig. 8. If convection is either more vigorous or the initial enthalpy content larger, the solidus may well retreat all the way back to the contact. Similar behavior has been found in the solidification of a single component melt cooled from above with internal heat generation [51], where the oscillations are sustained by the ongoing generation of internal heat. Only one oscillation is possible in the coupled solidification/melting system as the enthalpy

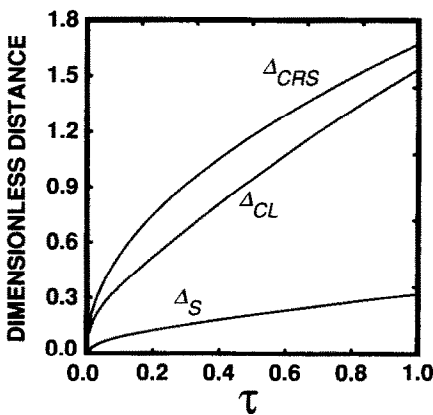


FIG. 6. Positions of the solidus in the initially molten region, country rock and the position of the convective liquidus, closed system case, equation (28). $\Gamma = 0.88$.

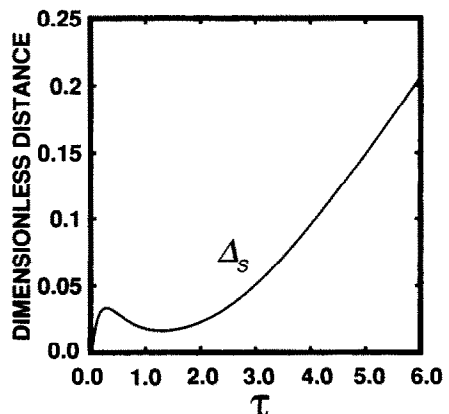


FIG. 8. Position of the solidus isotherm, closed system, $\Gamma = 0.68$.

content of the melt reservoir decays monotonically (Fig. 8).

4. CONCLUSIONS

Among the most important differences between single and multicomponent systems is the rheological partitioning that occurs during solidification or melting [19]. Changes in solid fraction yield concomitant changes in rheology which in turn dictates the driving temperature differences for thermal convection, and the time scales and manner in which convective structures are organized. This is particularly critical in geological materials where large changes in melt fraction can occur over relatively small temperature differences (Fig. 2). The method of weighted residuals provides a ready means of modeling such diverse behavior as the domain can be subdivided such that the solid fraction can be written as a continuous function across a subdomain; jump conditions can be accommodated by matching at the domain boundary [39]. Such an approach has been adapted to the problem of coupled solidification and melting in the presence of thermal convection.

The distribution of solids in the multicomponent system differs substantially from the single component system (Fig. 4); this will influence both the rate of heat transfer and the time scales of macrosegregation. The thermal flux from convection can induce a cycle of melting back in the solidified portion, the time scales associated with this melting back will depend on the value of the convective liquidus, the heat transfer coefficient and the enthalpy content of the melt body for the closed system case. An effective Nusselt number, defined as the ratio of the thermal flux at the contact in the presence of convection to that of conduction shows a simple time dependence and a maximum of ~ 1.35 .

This contribution presents some of the generic time-dependent behavior of a coupled solidification/melting system for a single parameter set. It is to be expected that variations in the physical properties will yield a stretching of the curves given in Figs. 3–8, however the basic morphology of the solutions to equations (5)–(25) will be the same. More complex systems are currently the subject of experimental and numerical analysis.

Acknowledgements—This work was supported by the U.S. Department of Energy under contract to Pacific Northwest Laboratory DE-AC06-76RLO 1830 and National Science Foundation Grants OCE-9000993 and EAR-9019217. Dr M. Murphy of Battelle is thanked for bringing the paper of Shekler to my attention.

REFERENCES

1. L. S. Yao and J. Prusa, Melting and freezing, *Adv. Heat Transfer* **19**, 1–95 (1989).
2. R. Viskanta, Heat transfer during melting and solidification of metals, *J. Heat Transfer* **110**, 1205–1219 (1988).
3. D. Loper, *Structure and Dynamics of Partially-solidified Systems*, NATO ASI Series, Series E, No. 125. Martinus Nijhoff, Dordrecht, The Netherlands (1987).
4. F. B. Cheung and M. Epstein, Solidification and melting in fluid flow. In *Advances in Transport Processes* (Edited by A. S. Majumdar and R. A. Mashelkar), pp. 35–117. Wiley, Eastern, New Delhi (1984).
5. R. N. Hills, D. E. Loper and P. H. Roberts, A thermodynamically consistent model of a mushy zone, *Q. J. Appl. Math.* **36**, 505–538 (1983).
6. R. N. Hills and P. H. Roberts, A generalized Scheil–Phann equation for a dynamical theory of a mushy zone, *Int. J. Non-Linear Mech.* **23**, 327–339 (1988).
7. R. N. Hills and P. H. Roberts, On the formulation of diffusive mixture theories for two-phase regions, *J. Engng Math.* **22**, 93–106 (1988).
8. R. N. Hills and P. H. Roberts, On the use of Fick's law in regions of mixed phase, *Int. Commun. Heat Mass Transfer* **15**, 113–119 (1988).
9. D. E. Loper and P. H. Roberts, A Boussinesq model of a slurry. In *Structure and Dynamics of Partially Solidified Systems* (Edited by D. E. Loper), pp. 291–323. Martinus Nijhoff, Dordrecht, The Netherlands (1987).
10. P. H. Roberts and D. E. Loper, Dynamical processes in slurries. In *Structure and Dynamics of Partial Solidified Systems* (Edited by D. E. Loper), pp. 229–290. Martinus Nijhoff, Dordrecht, The Netherlands (1987).
11. D. E. Loper and P. H. Roberts, On the motion of an iron-alloy core containing a slurry. I. General theory, *Geophys. Astrophys. Fluid Dynam.* **9**, 298–321 (1978).
12. W. D. Bennon and F. P. Incropera, A continuum model for momentum, heat and species transport in binary solid–liquid phase change systems—I. Model formulation, *Int. J. Heat Mass Transfer* **30**, 2161–2170 (1987).
13. C. Beckermann and R. Viskanta, Double-diffusive convection during dendritic solidification of a binary mixture, *PCH* **10**, 195–213 (1988).
14. M. S. Christenson and F. P. Incropera, Solidification of an aqueous ammonium chloride solution in a rectangular cavity—I. Experimental study, *Int. J. Heat Mass Transfer* **32**, 47–68 (1989).
15. C. Beckermann and R. Viskanta, An experimental study of melting of binary mixtures with double-diffusive convection in the liquid, *Exp. Thermal Fluid Sci.* **2**, 17–26 (1989).
16. B. D. Marsh, On convective style and vigor in sheet-like magma bodies, *J. Petrology* **30**, 479–530 (1989).
17. W. D. Bennon and F. P. Incropera, A continuum model for momentum, heat and species transport in binary solid–liquid phase change systems—II. Application to solidification in a rectangular cavity, *Int. J. Heat Mass Transfer* **30**, 2171–2187 (1987).
18. M. E. Thompson and J. Szekeley, Density stratification due to the counterbuoyant flow along a vertical crystallization front, *Int. J. Heat Mass Transfer* **32**, 1021–1035 (1989).
19. G. Brandeis and B. D. Marsh, The convective liquidus in a solidifying magma chamber: a fluid dynamic investigation, *Nature* **339**, 613–616 (1989).
20. R. M. German, The contiguity of liquid phase sintered microstructures, *Metall. Trans.* **16**, 1247–1252 (1985).
21. C. F. Miller, E. B. Watson and T. M. Harrison, Perspectives on the source, segregation and transport of granitoid magmas, *Trans. R. Soc. Edinburgh* **79**, 135–156 (1988).
22. A. A. Arzi, Critical phenomena in the rheology of partially melted rocks, *Tectonophysics* **44**, 173–184 (1978).
23. I. van der Molen and M. S. Paterson, Experimental deformation of partially-melted granite, *Contrib. Mineralogy Petrology* **70**, 299–318 (1979).
24. B. D. Marsh, Causes of magmatic diversity, *Nature* **333**, 397 (1988).
25. M. K. Smith, Thermal convection during the directional

- solidification of a pure liquid with variable viscosity, *J. Fluid Mech.* **188**, 547–570 (1988).
26. K. V. Cashman and B. D. Marsh, Crystal size distribution (CSD) in rocks and the kinetics and dynamics of crystallization, *Contrib. Mineralogy Petrology* **99**, 292–305 (1988).
 27. G. W. Bergantz and R. P. Lowell, The role of conjugate convection in magmatic heat and mass transfer. In *Structure and Dynamics of Partially Solidified Systems* (Edited by D. E. Loper), pp. 367–382. Martinus Nijhoff, Dordrecht, The Netherlands (1987).
 28. C. R. Carrigan, A two-phase hydrothermal cooling model for shallow intrusions, *J. Volc. Geothermal Res.* **28**, 175–192 (1986).
 29. Z. Zhang and A. Bejan, The problem of time-dependent natural convection melting with conduction in the solid, *Int. J. Heat Mass Transfer* **32**, 2447–2457 (1989).
 30. A. Bejan, Analysis of melting by natural convection in an enclosure, *Int. J. Heat Fluid Flow* **10**, 245–252 (1989).
 31. P. Jany and A. Bejan, Scaling theory of melting with natural convection in an enclosure, *Int. J. Heat Mass Transfer* **31**, 1221–1235 (1988).
 32. W.-Z. Cao and D. Poulikakos, Solidification of an alloy in a cavity cooled through its top surface, *Int. J. Heat Mass Transfer* **33**, 427–434 (1990).
 33. J. Szekely and A. S. Jassal, An experimental and analytical study of the solidification of a binary dendritic system, *Metall. Trans.* **9B**, 299–398 (1978).
 34. L. C. MacAuley and F. Weinberg, Liquid metal flow in horizontal rods, *Metall. Trans.* **4**, 2097–2106 (1973).
 35. T. W. Clyne, Modelling of heat flow in solidification, *Mater. Sci. Engr* **65**, 111–124 (1984).
 36. G. W. Bergantz and R. P. Lowell, Double-diffusive boundary layer convection in a porous medium and implications for fractionation in magma chambers, *EOS Trans. Am. Geophys. Un.* **66**, 361 (1985).
 37. C. F. Chen and S. Thangham, Effects of viscosity variation and cooling rates on crystallization and subsequent double-diffusive convection, *7th Int. Heat Transfer Conf.*, pp. 363–368 (1982).
 38. S. Tait and C. Jaupart, Compositional convection in viscous melts, *Nature* **338**, 571–574 (1989).
 39. V. R. Voller, A heat balance integral method for estimating practical solidification parameters, *IMA J. Appl. Math.* **35**, 223–232 (1985).
 40. R. H. Tien and G. E. Geiger, A heat-transfer analysis of a binary eutectic system, *J. Heat Transfer* **89**, 230–234 (1967).
 41. S. D. Howison, Similarity solutions to the Stefan problem and the binary alloy problem, *IMA J. Appl. Math.* **40**, 147–161 (1988).
 42. G. W. Bergantz, Underplating and partial melting: implications for melt generation and extraction, *Science* **245**, 1093–1095 (1989).
 43. B. A. Finlayson, *The Method of Weighted Residuals and Variational Principals*. Academic Press, New York (1972).
 44. J. M. Hill, *One-dimensional Stefan Problems: an Introduction*. Longman, Essex (1987).
 45. T. R. Goodman, Application of integral methods to transient non-linear heat transfer, *Adv. Heat Transfer* **1**, 51–122 (1964).
 46. V. R. Voller, A heat balance integral method based on an enthalpy formulation, *Int. J. Heat Mass Transfer* **30**, 604–607 (1987).
 47. T. W. Clyne and W. Kurtz, Solute redistribution during solidification with rapid solid state diffusion, *Metall. Trans. A* **12**, 965–971 (1981).
 48. C. A. Shekler and D. R. Dinger, Effect of particle size distribution on the melting of soda-lime-silica glass, *J. Am. Ceram. Soc.* **73**, 24–30 (1990).
 49. B. D. Marsh, Crystal capture and retention in convecting magma, *Geol. Soc. Am. Bull.* **100**, 1720–1737 (1988).
 50. J. J. Dongarra and E. Grosse, Distribution of mathematical software via electronic mail, *Commun. ACM* **30**, 403–407 (1987).
 51. F. B. Cheung, Periodic growth and decay of a frozen crust over a heat generating liquid layer, *J. Heat Transfer* **103**, 369–375 (1981).

SOLIDIFICATION ET FUSION CONJUGUEE DANS DES SYSTEMES OUVERTS OU FERMES A PLUSIEURS COMPOSANTS

Résumé—A la base des technologies de changement de phase et des matériaux géologiques, on considère la solidification et la fusion variables de matériaux multicomposants à une dimension avec convection thermique ouverte ou fermée. La mise en échelle de la différence de température motrice pour la convection est fonction de la différence de température entre l'isotherme qui délimite une purée rigide d'une boue et la température de l'écoulement libre. L'évolution temporelle des zones solides et purées pour le cas du système ouvert multicomposant est qualitativement similaire au cas d'un composant unique. Les flux thermiques maximums sont jusqu'à 1,35 fois ceux pour solidification/fusion conductives couplées. Le cas du système convectif fermé conduit à deux possibilités : une progression monotone de la solidification ou une oscillation dans les positions des isothermes dépendantes du rapport du coefficient de transfert thermique au contenu enthalpique et de la géométrie du réservoir du fluide.

GEKOPPELTE ERSTARRUNGS- UND SCHMELZVORGÄNGE IN OFFENEN UND GESCHLOSSENEN MEHRKOMponentensystemen

Zusammenfassung—Angeregt durch Technologien mit Phasenwechsel bei geologischen Materialien werden die zeitabhängigen gekoppelten Erstarrungs- und Schmelzvorgänge von Mehrkomponentensystemen betrachtet. Die eindimensionale Betrachtung umfaßt offene und geschlossene Systeme mit thermisch bedingter Konvektion. Die Größe der treibenden Temperaturdifferenz für die Konvektion ist eine Funktion der Temperaturdifferenz zwischen der Isothermen, welche die feste breiige Zone von der flüssigen breiigen abgrenzt, und der Temperatur der freien Strömung. Die zeitliche Bildung von festen und breiigen Zonen ist für ein offenes Mehrkomponentensystem qualitativ sehr ähnlich zu einem Einkomponentensystem. Der maximal übertragene Wärmestrom ist etwa 1,35-mal so groß wie beim gekoppelten Erstarrungs- und Schmelzvorgang mit Wärmeleitung. Der Fall des geschlossenen konvektiven Systems besitzt zwei mögliche Zustände: ein gleichmäßiges Fortschreiten des Erstarrungsvorgangs oder eine Oszillation der Isothermenpositionen, abhängig vom Verhältnis des Wärmeübergangskoeffizienten zur Enthalpie und Geometrie des Flüssigkeitsgebiets.

СОПРЯЖЕННЫЕ ПРОЦЕССЫ ПЕРЕНОСА ПРИ ЗАТВЕРДЕВАНИИ И ПЛАВЛЕНИИ В МНОГОКОМПОНЕНТНЫХ ОТКРЫТЫХ И ЗАМКНУТЫХ СИСТЕМАХ

Аннотация—Рассмотрены нестационарные сопряженные процессы в геологических материалах при наличии фазовых переходов (затвердевания и плавления) и тепловой конвекции в открытых и замкнутых системах. Определение масштаба разности температур, обуславливающей конвекцию, зависит от разности температур между изотермой, разграничивающей области жесткого пористого состояния и состояния суспензии, и свободным потоком. В случае многокомпонентной незамкнутой системы временная эволюция твердой и пористой зон качественно сходна с однокомпонентным случаем. Максимальные скорости теплопереноса в 1,35 раз выше, чем при процессах кондуктивного затвердевания и плавления. Для замкнутой системы при наличии конвекции возможны два результата: монотонное развитие затвердевания или колебание расположений изотерм в зависимости от отношения коэффициента теплопереноса к теплосодержанию и от геометрии объема жидкости.